

MICROCOPY RESOLUTION TEST CHART
NATIONAL BUREAU OF STANDARDS-1963-A

UNCLASSIFIED

2

AD-A150 881 REPORT DOCUMENTATION PAGE

1a. REPORT SECURITY CLASSIFICATION		1d. RESTRICTIVE MARKINGS	
2a. SECURITY CLASSIFICATION AUTHORITY		3. DISTRIBUTION AVAILABILITY OF REPORT Approved for public release; distribution unlimited.	
2b. DECLASSIFICATION/DOWNGRADING SCHEDULE			
4. PERFORMING ORGANIZATION REPORT NUMBER(S)		5. MONITORING ORGANIZATION REPORT NUMBER(S) AFOSR-TR- 85-0159	
6a. NAME OF PERFORMING ORGANIZATION Dept. of Medication Engrin. Auburn Univ. City	6b. OFFICE SYMBOL (If applicable)	7a. NAME OF MONITORING ORGANIZATION AFOSR/NE	
6c. ADDRESS (City, State and ZIP Code) 247 Williams Hall Auburn Univ., AL 36849		7b. ADDRESS (City, State and ZIP Code) Bldg 410 Bolling AFB, DC 20332-6448	
8a. NAME OF FUNDING/SPONSORING ORGANIZATION AFOSR	8b. OFFICE SYMBOL (If applicable) NE	9. PROCUREMENT INSTRUMENT IDENTIFICATION NUMBER AFOSR-83-0168	
8c. ADDRESS (City, State and ZIP Code) Bldg 410 Bolling AFB, DC 20332-6448		10. SOURCE OF FUNDING NOS. PROGRAM ELEMENT NO. PROJECT NO. 61102F 2308	
11. TITLE (Include Security Classification) ORDERED CARBON METAL ALLOYS FOR EXTRATERRESTRIAL			
12. PERSONAL AUTHOR(S) POWER SYSTEMS B. A. Wier, N. H. Meiser, P. F. Gills, S. C. Su			
13a. TYPE OF REPORT Technical	13b. TIME COVERED FROM <u>APR 83</u> TO <u>APR 84</u>	14. DATE OF REPORT (Yr., Mo., Day) July 31, 1984	15. PAGE COUNT 55
16. SUPPLEMENTARY NOTATION			
17. COSATI CODES FIELD GROUP SUB GR.		18. SUBJECT TERMS (Continue on reverse if necessary and identify by block number) Cluster-Variation, Concentration Waves and Band Theory.	
19. ABSTRACT (Continue on reverse if necessary and identify by block number) Theoretical methods of predicting ordering parameters of carbon metal based systems have been investigated. Preliminary methods of calculating the critical ordering temperature, and the maximum degree of order have been used to examine the characteristics of C-Zr, C-Mo, C-Ti and C-V systems. Based upon these calculations, the C-Ti system has been chosen as the most promising system in which the ultrahigh strength, ductility and temperature resistance, properties desired for space power generation materials, can be obtained. Fifteen titanium based alloys have been manufactured using an arc melting furnace to compare experimentally the effect of carbon content on the ordering parameters of carbon metal alloys with theoretical predictions. The alloys produced contained between 0 and 53 atom percent (0 to 22 weight percent) carbon. This first group of alloys did not contain transition and rare earth additions required for ductility improvement. This will allow an unperturbed comparison of ordering parameter theory with experimental results. Optical metallography and			
20. DISTRIBUTION/AVAILABILITY OF ABSTRACT UNCLASSIFIED/UNLIMITED <input checked="" type="checkbox"/> SAME AS RPT. <input type="checkbox"/> DTIC USERS <input type="checkbox"/>		21. ABSTRACT SECURITY CLASSIFICATION UNCLASSIFIED	
22a. NAME OF RESPONSIBLE INDIVIDUAL JOSEPH W. EAGER, Capt, USAF		22b. TELEPHONE NUMBER (Include Area Code) (202) 767-4932	22c. OFFICE SYMBOL NE

**DTIC
SELECTED
MAR 06 1985
S E**

UNCLASSIFIED

SECURITY CLASSIFICATION OF THIS PAGE

Analysis of the castings completed in June 1964 with interesting results. The castings containing 10 atomic percent and 15 atomic percent titanium to 20 weight percent carbon. These alloys were found to contain significant amounts of phases not predicted from the phase diagrams. X-ray diffraction tests are being conducted to identify these constituents.

An additional casting has been manufactured using a new induction generator purchased under the contract. Two compression tests have been conducted on specimens cut from these melts. One of the specimens was a Ti-5 w/c carbon alloy which was found to have a yield strength of 100 ksi, ultimate tensile strength of 160 ksi and 5.5% strain to fracture at room temperature. This alloy has a melting temperature of nearly 2000°C compared to traditional Ti alloys such as Ti-6Al-4V which has a melting temperature of 1650°C, UTS of 130 ksi and elongation of 12% in the forged bar condition.

Original supplied keywords include:

See 1-1-1-1

UNCLASSIFIED

SECURITY CLASSIFICATION OF THIS PAGE

AFOSR-TR- 85 - 0159

ORDERED CARBON - METAL ALLOYS FOR
EXTRATERRESTRIAL POWER SYSTEMS

Interim Progress Report - First Year

AFOSR Grant: 83-0168

B. A. Chin
N. H. Madsen
P. F. Gills
S. C. Su

Department of Mechanical Engineering
Auburn University, AL 36849
Phone: (205) 826-4820

Accession For	
NTIS GRA&I	<input checked="" type="checkbox"/>
DTIC TAB	<input type="checkbox"/>
Unannounced	<input type="checkbox"/>
Justification	
By	
Distribution/	
Availability Codes	
Dist	Avail and/or Special
A-1	



Approved for public release;
distribution unlimited.

Table of Contents

I. Summary of Progress	1
II. Objective	2
III. Introduction	3
IV. Progress During First Year of Project	6
A. Theoretical Progress	7
i. Introduction	7
ii. Bragg-Williams, Kirkwood, Quasichemical Methods	10
iii. Cluster-Variation, Concentration Waves and Band Theory	27
iv. Ordering Energy	35
v. Summary	38
B. Experimental Progress	40
V. Conclusions	52
VI. References	53

AIR FORCE OFFICE OF SCIENTIFIC RESEARCH (AFSC)
NOTICE OF TRANSMITTAL TO DTIC
This technical report has been reviewed and is
approved for public release (unclassified).
Distribution is unlimited.
MATTHEW J. KERPER
Chief, Technical Information Division

I. SUMMARY OF PROGRESS

During the first year of the contract, theoretical methods of predicting ordering parameters of carbon metal based systems have been investigated. Preliminary methods of calculating the critical ordering temperature, and the maximum degree of order have been used to examine the characteristics of C-Zr, C-Mo, C-Ti and C-V systems. Based upon these calculations, the C-Ti system has been chosen as the most promising system in which the ultrahigh strength, ductility and temperature resistance, properties desired for space power generation materials, can be obtained.

Fifteen titanium based alloys have been manufactured using an arc melting furnace to compare experimentally the effect of carbon content on the ordering parameters of carbon metal alloys with theoretical predictions. The alloys produced contained between 0 and 53 atom percent (0 to 22 weight percent) carbon. This first group of alloys did not contain transition and rare earth additions required for ductility improvement. This will allow an unperturbed comparison of ordering parameter theory with experimental results. Optical metallography and hardness tests have been completed on these alloys with interesting results for alloys containing between 35 and 53 atomic percent (12 to 22 weight percent) carbon. These alloys were found to contain significant amounts of phases not predicted from the phase diagrams. X-ray diffraction tests are being conducted to identify these constituents.

An additional ten alloys have been manufactured using a new induction generator purchased under the contract. Two compression tests have been conducted on specimens cut from these melts. One of these specimens was a Ti-5 w/o carbon alloy which was found to have a yield strength of 100 ksi, ultimate tensile strength of 164 ksi and 5.4% strain to fracture at room temperature.

This alloy has a melting temperature of nearly 2000°C compared to traditional Ti alloys such as Ti-6Al-4V which has a melting temperature of 1650°C, UTS of 130 ksi and elongation of 4% in the forged bar condition.

The project is currently on schedule and within budget.

II. OBJECTIVE

The objective of the proposed research is to investigate a new class of materials composed of 30-60 atomic percent carbon (C-Mo, C-Zr, C-V C-Ti) for ultrahigh temperature applications in space power systems. The proposed alloy systems exhibit melting temperatures in excess of 2500°C and form long range ordered structures which are expected to yield materials with exceptional high temperature strength and irradiation resistance.

III. INTRODUCTION

The generation of power in space by methods other than direct conversion (photovoltaic) will require new concepts in materials to obtain optimum performance. Traditional materials used in the construction of land based power systems such as zircaloy, stainless steel, and in some exotic applications, Nb and V steels, do not have the necessary combined ultrahigh temperature strength, irradiation resistance, and strength to weight ratios that are required. The space reactor will operate in a near perfect vacuum, eliminating oxidation problems which plague many high temperature materials (Mo, V, etc.). However, sublimation of the materials (vaporization at high temperatures) will become a controlling factor. In space, the rejection of heat must occur by radiation of energy to the environment, requiring temperatures of 1000°C or greater for thermodynamic efficiency. Additionally, the materials are required to withstand the radiation of the nuclear core (be resistant to irradiation induced densification, swelling and creep) and be lightweight for transportation into space.

Viewing the above general requirements, carbon based materials (C materials) are a superb candidate for development. C fiber - C matrix materials have been highly successful on the space shuttle where they have been used for components ranging from cargo bay doors to high temperature motor casings. Such materials, however, are not suited for applications which require exposure to nuclear radiation. Testing in the high temperature gas cooled reactor program has identified two problems with C materials.

The first is the permeability of the C material to radioactive fission gases [1,2]. Despite the development of ultrahigh density C materials, special C coatings, and differential pressurization of components, leakage of C clad fuel occurs after very short neutron exposures ($\phi t < 1 \times 10^{22} \text{n/cm}^2$).

Heat pipe components, fabricated from pure C or C composite materials, would therefore be unable to maintain proper partial pressures for operation. The second problem results from volumetric changes (densification) that occur in C materials upon neutron irradiation [1]. These changes are highly orientation dependent. The C fibers, which contain material with the basal planes aligned perpendicular to the stress axes, undergo a substantially different volumetric change than the matrix material, leading to the generation of high internal stress, cracking and ultimate failure. A class of materials which promise to overcome the above described problems is ordered C-metal alloys. Ordered alloys offer many potential advantages over conventional alloys at elevated temperatures [2-5]. The atomic ordering produces a pronounced increase in the work hardening [5-9], improves the fatigue resistance [10], and retards, because of stronger binding and closer packing of atoms, most thermally activated processes such as creep and grain growth [11]. In addition, the strength of ordered alloys is less sensitive to temperature than conventional disordered alloys. In fact some alloys show an increase rather than a decrease in strength with increasing temperature up to the critical ordering point [12]. The critical ordering point is the temperature at which the material reverts from a defined periodic arrangement of alloying elements to the random arrangement found in conventional materials. Electron, ion bombardment and recent neutron irradiation results show the long range ordered (LRO) alloys to be highly swelling resistant [13-15].

Despite the above advantages, the LRO alloys have seen only limited application because of a lack of ductility associated with the ordered state [16-18]. Recently Liu and his coworkers at ORNL have succeeded in producing $(\text{Fe, Ni})_3\text{V}$ long range ordered alloys which show tensile elongations greater

than 30% [19-21]. This has been achieved by controlling the ordered lattice structure through use of the e/a ratio or average electron density per atom outside the inert gas shell.

Ordered C-metal alloys represent a new approach which combines the desirable qualities of C (high temperature resistance, low weight, low vapor pressure) with the radiation and permeability resistance of ordered materials. These alloys, containing 30-60 atomic percent carbon, all exhibit melting temperatures in excess of 2500°C [22,23]. By careful control of the alloy composition, desirable ordered structures can be maintained at temperatures in excess of 0.7T_m (approx.1800°C). The alloys will be relatively lightweight, yet resistant to irradiation damage. Control of the ordered structure by modification of the e/a ratio will produce compositions with good ductility, strength, creep and fatigue properties. In addition, the C-metals will eliminate the permeability problem associated with pure C materials.

The objective of this research is to investigate the property-structure relationships of ordered C-metal alloys. These studies will provide a theoretical and experimental basis from which a future development program, leading to optimization and detailed characterization of ordered C-metal alloys, can be initiated.

IV. PROGRESS DURING FIRST YEAR OF THE PROJECT

The principal accomplishments during the first year of the project deal with both theoretical and experimental achievements. Based upon the initial proposed project plan, the research is on schedule. The work herein reported was performed by two graduate students seeking Master's of Science and Doctor of Philosophy degrees from our Department of Mechanical Engineering. Most of the work reported was performed by Pamela Gills who began research on the project in June 1983. S. C. Su joined the research team in March 1984 and as such his contributions to the reported progress to date are minimal.

Approximately twenty-five percent of the first year's effort was spent setting up theoretical models and analyzing the C-Ti, C-V, C-Mo and C-Zr systems for the alloys with the highest probability for success. Fifty percent of the expended effort was required to melt and examine the initial C-Ti alloys and the remaining twenty-five percent was used setting up equipment. The following two sections describe the progress made to date in the theoretical and experimental areas.

A. Theoretical Progress

i. Introduction

There are a number of theoretical models available which allow the calculations of the critical ordering temperature, maximum degree of order and specific heat as a function of temperature for ordered alloy systems. It is the objective of this research to apply these theories to the Ti-C alloy system. The results of the above computations will provide a theoretical basis upon which the most promising alloy systems and ranges of compositions can be chosen for melting and experimentation under Activity II. It is hoped that before alloying additions are made that we will be able to extend these theoretical calculations to ternary systems [24].

This section documents the work accomplished so far in these efforts and the work planned for the future. Included in the report is a brief synopsis of some of the theoretical models of ordering found in the literature, and a discussion of problems encountered in applying them to our system.

Unlike conventional alloys, which form a random mixture of atoms on lattice sites, long range ordered (LRO) alloys exhibit periodic arrays which form an ordered crystal structure. In general, unlike atoms tend to be closer together and like atoms further apart. The tendency to order increases with decreasing temperatures, therefore, the ordered arrangement of atoms must be more stable or energetically favorable at lower temperatures than a random distribution. For this to be true, the attraction between unlike atoms must be stronger than the attraction between like atoms. As the temperatures of the alloy increases the energy of thermal vibration increases and when this exceeds the so called ordering energy the atoms have sufficient energy to

redistribute themselves into a disordered or random mixture; it is at this point that the disordered structure becomes the stable configuration. Thus, we expect a transition temperature at which the ordered phase becomes unstable. This transition temperature, the critical temperature, T_c , is analogous to the Curie temperature in ferromagnetism. One of our objectives was the prediction of the critical ordering temperature for various carbon alloys. To make this prediction, a review of the various theoretical models of ordering was undertaken. This review is summarized in what follows. Above the critical temperature the alloy is completely disordered. Once the critical temperature is reached atomic ordering begins and at each temperature below the critical temperature (after suitable heat treatment) an equilibrium degree of order will be reached. Thus, at the stoichiometric composition of the alloy, the equilibrium degree of order at high temperatures will be zero and at 0°K the alloy will be completely ordered. Alloys which are not stoichiometric will not reach perfect order, but will have a characteristic maximum degree of order depending on the composition.

The first suggestion that some alloys can exhibit an ordered structure, or super-lattice was put forth in 1919 by Tammann [25] after his observations in the Cu-Au system. Since that time a number of efforts have been made to theoretically describe and predict the cooperative phenomena of ordering [26].

The first successful theory of the stability of superlattices, as a function of temperature, was developed by Bragg and Williams [27]. Later, Bethe [28] developed a more refined method, which was extended by several authors. Neither one of these methods were very clear about the assumptions which were made; Kirkwood [29] remedied this by developing a theory based entirely on the standard concepts of statistical mechanics. The quasichemical method was

developed also at this time by Guggenheim [30] and was later shown to be equivalent to Bethe's method [31].

The more recent past has seen the development of several more theories, including: the Cluster-variation method developed by Takagi [32], Kikuchi [33], Yang, Li [34] and Hill [35], the method of concentration waves [11], and a band theory model [37]. In addition to these, numerical methods based on the random walk or Monte Carlo Method [38] have been developed.

Except for band theory, all of the above models require the interaction or ordering energies of the alloy,

$$V^i = V_{AA}^i + V_{BB}^i - V_{AB}^i \quad (1)$$

where the superscript $i=1$ denotes nearest neighbors, $i=2$ denotes next nearest neighbors, etc., and the subscripts denote which pair of atoms the energy $V_{\alpha\beta}$ represents. Unfortunately, this energy parameter is hard to come by. This will be discussed later.

ii. Bragg-Williams, Kirkwood, Quasichemical Methods

In order to specify the degree of order of the atomic arrangement over the lattice sites Bragg and Williams introduced the long range order parameter s in their original paper [27]. When perfect order is achieved in a binary alloy of components A and B the lattice sites occupied by A atoms are called α sites and those occupied by B atoms are called β sites. Let N be the total number of atoms (A and B) and thus the total number of lattice sites, (i.e. no vacancies); and F_A and F_B (where $F_B = 1 - F_A$), be the fraction of A and B atoms in the alloy respectively. Also let the fraction of α sites occupied by A atoms be denoted by r_α , (right atoms), the fraction of α sites occupied by B atoms be w_α , where $w_\alpha = 1 - r_\alpha$ and similarly r_β and $w_\beta = 1 - r_\beta$ represent the rightly and wrongly occupied β sites. The long range order parameter s may now be defined as

$$s = \frac{r_\alpha - F_A}{1 - F_A} = \frac{r_\beta - F_B}{1 - F_B} \quad (2)$$

Thus, s is defined as unity for perfect order and vanishes in the completely disordered state.

Now, let Q be the total number of all types of pairs in the lattice and each atom be surrounded by z nearest neighbors, thus

$$Q = \frac{z}{2} N \quad (3)$$

Also let the number of pairs, which are AA, BB and AB be denoted by Q_{AA} , Q_{BB} , Q_{AB} respectively. Consider an alloy with $F_A N$ α sites and $F_B N$ β sites, then according to equation (2) the average number of A and B atoms on α and β sites are as follows [26]:

$$\begin{aligned}
\text{A atoms on } \alpha \text{ sites: } r_{\alpha} F_{\alpha N} &= (F_A + F_{\beta s}) F_{\alpha N}, \\
\text{A atoms on } \beta \text{ sites: } w_{\beta} F_{\beta N} &= (1 - s) F_A F_{\beta N}, \\
\text{B atoms on } \alpha \text{ sites: } w_{\alpha} F_{\alpha N} &= (1 - s) F_{\beta} F_{\alpha N}, \\
\text{B atoms on } \beta \text{ sites: } r_{\beta} F_{\beta N} &= (F_{\beta} + F_{\alpha s}) F_{\beta N}.
\end{aligned} \tag{4}$$

The number $g(s)$, of distinguishable arrangements or configurations for a given state s is then

$$g(s) = \frac{[F_{\alpha N}]!}{[(F_A + F_{\beta s}) F_{\alpha N}]! [(1-s) F_A F_{\beta N}]!} \cdot \frac{[F_{\beta N}]!}{[(1-s) F_A F_{\beta N}]! [F_{\beta} + F_{\alpha s}] F_{\beta N}]!} \tag{5}$$

Assuming, approximately that the lattice vibrations are independent of the configuration of the atoms in the lattice, the partition function in the canonical ensemble may be written as

$$Z(T, s) = \sum_{\tau} e^{-W_{\tau}/KT} \tag{6}$$

where T is the absolute temperature, s is the long range order, K is the Boltzmann constant and W_{τ} is the configurational energy of the state τ . The summation extends over all the states τ of a given order s .

Our knowledge of W_{τ} is scant at best at this time and is approximated here as consisting mainly of the interaction energies of pairs of nearest neighbors. These energies as identified in eq.(1) are V_{AA} , V_{BB} , V_{AB} , corresponding to nearest neighbor pairs Q_{AA} , Q_{BB} , Q_{AB} respectively. Therefore the configurational energy is roughly given by

$$W_{\tau} = - (Q_{AA} V_{AA} + Q_{BB} V_{BB} + Q_{AB} V_{AB}), \tag{7}$$

for any specified configuration τ .

The configurational free energy $F(s)$ is given by

$$F(s) = - kT \ln(Z(T, s)) \tag{8}$$

and once this is minimized the equilibrium value of s will be determined. The corresponding energy of the alloy is

$$E(s) = W(s) = \frac{\sum_{\tau} W_{\tau} e^{-W_{\tau}\beta}}{\sum_{\tau} e^{-W_{\tau}\beta}}, \quad (9)$$

where β is $1/KT$.

Now, using the conventional procedures of statistical mechanics, we define $U(s)$ by the relation

$$\sum_{\tau} e^{-W_{\tau}\beta} = g(s)e^{-U(s)\beta} \quad (10)$$

here $g(s)$ is the same as in eq. (5). Now, β can be written as

$$F(s) = U(s) - KT \ln(g(s)), \quad (11)$$

and the energy of the alloy can be written as

$$E(s) = \frac{\partial}{\partial(1/T)} \frac{U(s)}{T}. \quad (12)$$

The above equations for the free energy and internal energy define the thermodynamics of the system [26]. All that is left to do is to calculate the partition function. This however has proved illusive and various approximations have been made to it, the first of which was the Bragg-Williams approximation [27]. Their approximation consists of replacing the true value of w_{τ} for each configuration of s by the simple average $\langle w_{\tau} \rangle$ of all states belonging to a given s ,

$$\langle w_{\tau} \rangle = - \{ \langle Q_{AA} \rangle V_{AA} + \langle Q_{BB} \rangle V_{BB} + \langle Q_{AB} \rangle V_{AB} \}, \quad (13)$$

where $\langle Q_{AA} \rangle$, $\langle Q_{BB} \rangle$ and $\langle Q_{AB} \rangle$ are the simple averages of the number of pairs of each kind in each state τ of s . Consider $\langle Q_{AA} \rangle$, AA pairs may result from two arrangements: (1) one A atom on an α site and the other one on a β site, and

(2) both atoms on β sites. On the average there are $F_A N(F_A + F_B s)$ α sites occupied by A atoms each having $z(1-s)F_A$ neighboring β sites occupied by A atoms. There are then $zNF_A^2(1-s)(F_A + F_B s)$ AA pairs of type (1). The number of AA pairs with both atoms on β sites is $\frac{1}{2}zNF_A^2(F_B - F_A)(1-s)^2$ [26]. Therefore,

$$\begin{aligned} \langle Q_{AA} \rangle &= zNF_A^2(1-s)(F_A + F_B s) + \frac{1}{2}zNF_A^2(F_B - F_A)(1-s)^2 \\ &= \frac{1}{2}zN(F_A^2 - F_A^2 s^2), \end{aligned} \quad (14)$$

and similarly,

$$\begin{aligned} \langle Q_{BB} \rangle &= \frac{1}{2}zN(F_B^2 - F_A^2 s^2) \\ \langle Q_{AB} \rangle &= \frac{1}{2}zN(2F_A F_B + 2F_A s^2). \end{aligned}$$

Substituting equations (14) into (13) leads to

$$\begin{aligned} \langle W_T \rangle &= \frac{Nz}{2} (F_A^2 V_{AA} + 2F_A F_B V_{AB} + F_B^2 V_{BB}) \\ &\quad - \frac{Nz}{2} F_A^2 (2V_{AB} - V_{AA} - V_{BB}) s^2. \end{aligned} \quad (15)$$

Since $\langle W_T \rangle$ is independent of temperature in this approximation, by equations (10) and (12)

$$\langle W_T \rangle = E(s) = U(s) \quad (16)$$

Thus, the configurational free energy becomes

$$\begin{aligned} F(s) - F(0) &= NKT [F_A(F_A + F_B s) \ln \{F_A(F_A + F_B s)\} \\ &\quad + F_B(F_B + F_A s) \ln \{F_B(F_B + F_A s)\} \\ &\quad + 2F_A F_B (1-s) \ln \{F_A F_B (1-s)\} \\ &\quad - 2F_A \ln F_A - 2F_B \ln F_B] - NzVF_A^2 s^2 \end{aligned} \quad (17)$$

after using the expression for $g(s)$ in eq. (5) and eq. (15) for the energy in eq(11), where V is V^1 as defined in equation 1, in the nearest neighbor approximation. For the alloy of composition $F_A = F_B = \frac{1}{2}$

this expression reduces to

$$F(S) - F(1) = \frac{N}{2} KT \{ (1+s) \ln(1+s) + (1-s) \ln(1-s) - 2 \ln 2 \} + \frac{1}{4} NzV(1-s^2). \quad (18)$$

The equilibrium state of the configuration in the alloy is found by minimizing the free energy. Thus, the condition

$$\frac{\partial F}{\partial s} = 0 \quad (19)$$

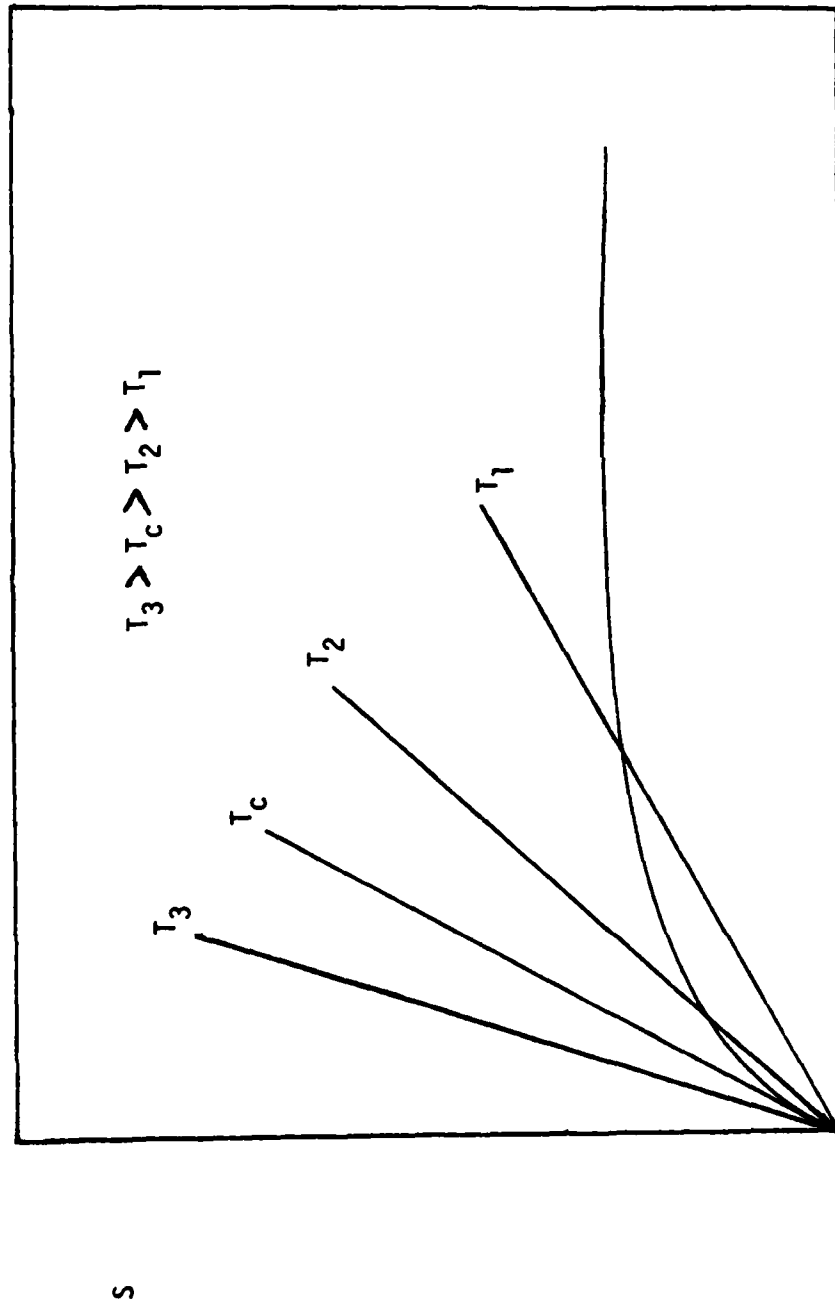
gives
$$s = \tanh \frac{zV}{2KT} s. \quad (20)$$

This equation determines the equilibrium value of s as a function of T . The above equation can be decomposed into

$$s = \tanh X \text{ and } s = \frac{2KT}{zNX}. \quad (21)$$

When these two equations are plotted as a function of X the intersection of the curves give the equilibrium value of s at T (see Figure 1). There are two solutions of (21), one at $s=0$ and one at $s>0$ for all T less than some T_c . The solution $s=0$ corresponds to the maximum free energy or the unstable state of order, whereas the solution of $s>0$ corresponds to the minimum free energy of equilibrium value of order. The solution of $s>0$ indicates the existence of the ordered state at temperatures below a critical value. The value of s decreases very slowly at first, then as the temperature continues to increase drops off abruptly at T_c , and vanishes at all temperatures greater than T_c . The critical temperature is found by the conditions

$$\frac{\partial F}{\partial s} = \frac{\partial^2 F}{\partial s^2} = s = 0. \quad (22)$$



X

Figure 1: Determination of S at T from equation 21.

These conditions lead to

$$KT_c = \frac{zV}{2} \quad (23)$$

for the critical temperature of an alloy with composition $F_A = F_B = 1/2$.

A higher approximation, developed by Kirkwood [29], is one which takes into account, on the average, the energy spread of W_τ for a given s around its average value $\langle W_\tau \rangle$. Although it is not possible to know the actual distribution of W_τ we can find the moments of deviations from $\langle W_\tau \rangle$. We write equation (10) as

$$U(s)/KT = \ln[g(s)] - \ln \left[\sum_{\tau} e^{-W_\tau/KT} \right] \quad (24)$$

and expanding the exponentials,

$$U(s)/KT = - \ln 1 - \frac{\langle W_\tau \rangle}{KT} + \frac{1}{2!} \frac{\langle W_\tau^2 \rangle}{(KT)^2} - \frac{1}{3!} \frac{\langle W_\tau^3 \rangle}{(KT)^3} + \dots \quad (25)$$

where $\langle W_\tau^n \rangle = \frac{g(s)}{\sum_{\tau=1} g(s)} \frac{W_\tau^n}{g(s)}$.

Upon further expansion of the logarithm above, $U(s)$ can be written as

$$U(s) = \langle W_\tau \rangle - \frac{1}{2!} \frac{1}{KT} \{ \langle W_\tau^2 \rangle - \langle W_\tau \rangle^2 \} + \frac{1}{3!} \frac{1}{(KT)^2} \{ \langle W_\tau^3 \rangle - 3\langle W_\tau \rangle \langle W_\tau^2 \rangle + 2\langle W_\tau \rangle^3 \}, \quad (26)$$

where $\langle W_\tau^2 \rangle - \langle W_\tau \rangle^2 = \langle (W_\tau - \langle W_\tau \rangle)^2 \rangle$ is the second moment and $\langle W_\tau^3 \rangle - 3\langle W_\tau \rangle \langle W_\tau^2 \rangle + 2\langle W_\tau \rangle^3 = \langle (W_\tau - \langle W_\tau \rangle)^3 \rangle$ is the third.

Substituting $\langle W_\tau \rangle$ for the alloy $F_A = F_B = 1/2$ into the above equation gives $U(s)$,

$$U(s) = \frac{-Nz}{2} V_{AB} + \frac{1}{2} NzV \left\{ \frac{1}{2}(1-s^2) - \frac{V}{KT} \frac{1}{8} (1-s^2)^2 - \frac{V}{KT} \frac{1}{12} s^2 (1-s^2)^2 + \dots \right\}. \quad (27)$$

The free energy is found by substituting the above equation and equation (5) for $g(s)$, into equation (11),

$$F(s) - F(1) = \frac{N}{2} KT \left\{ (1+s) \ln(1+s) + (1-s) \ln(1-s) - 2 \ln 2 \right\} + \frac{N}{2} zV \left\{ \frac{1}{4}(1-s^2) - \frac{V}{KT} \frac{1}{8} (1-s^2)^2 - \frac{V}{KT} \frac{1}{12} s^2 (1-s)^2 + \dots \right\}. \quad (28)$$

The B-W solution corresponds to keeping only the first and second terms of the above equation and ignoring all higher order terms. Again the equilibrium value of s at T is found by minimizing $F(s)$,

$$\ln \frac{1+s}{1-s} = \frac{zV}{KT} s \left\{ 1 - \frac{V}{KT} \frac{1}{2} (1-s^2) + \frac{V}{KT} \frac{1}{6} (1-s^2)(1-3s^2) + \dots \right\}. \quad (29)$$

This function drops off much more rapidly at T_c compared to the B-W approximation and is almost identical to Bethe's and Guggenheims quasichemical model [26]. However, difference in the specific heats do arise. The critical temperature is again found by the condition of $\frac{\partial F}{\partial s} = \frac{\partial^2 F}{\partial s^2} = s = 0$, and is

$$2 \frac{KT_c}{zV} = 1 - \frac{1}{2} \frac{V}{KT_c} + \frac{1}{6} \frac{V}{KT_c} + \dots. \quad (30)$$

Kirkwoods solution has the advantages over Bragg and Williams in that it is easily adopted to different types of lattices and to nonstoichiometry. Also, in principle, it is possible to obtain any degree of accuracy; however, equation (30) tends to converge very slowly at temperatures below T_c and higher moments are necessary for reliable results.

Bethe's solution [28] has been shown to be equivalent to Guggenheim's quasichemical method of solution. His original model, as will be presented here, is basically a construction of the grand partition function for a small group of lattice sites in which the variables of temperature, volume and absolute activities play important roles. However, the original model was not constructed as a grand canonical ensemble, instead Bethe based his development on nearest neighbor interactions and the short range order parameter σ . The short range order parameter, as defined by Bethe, is not based on α and β sites in the lattice but on the configuration of nearest neighbors. This parameter measures the way in which, on the average, each atom is surrounded by its neighbors, or the extent of local order. The short range order is defined as

$$\sigma = \frac{(q - q_r)}{q_m - q_r}, \quad (31)$$

where $q = Q_{AB}/Q$, q_m is the maximum value of q and q_r is the value of q in the disordered state. Here, the limits of zero and one are obtained for complete disorder and order respectively, as for the long range order.

Now, we select an arbitrary group of sites for consideration on the basis of nearest neighbor interactions, consider for example Figure 2.

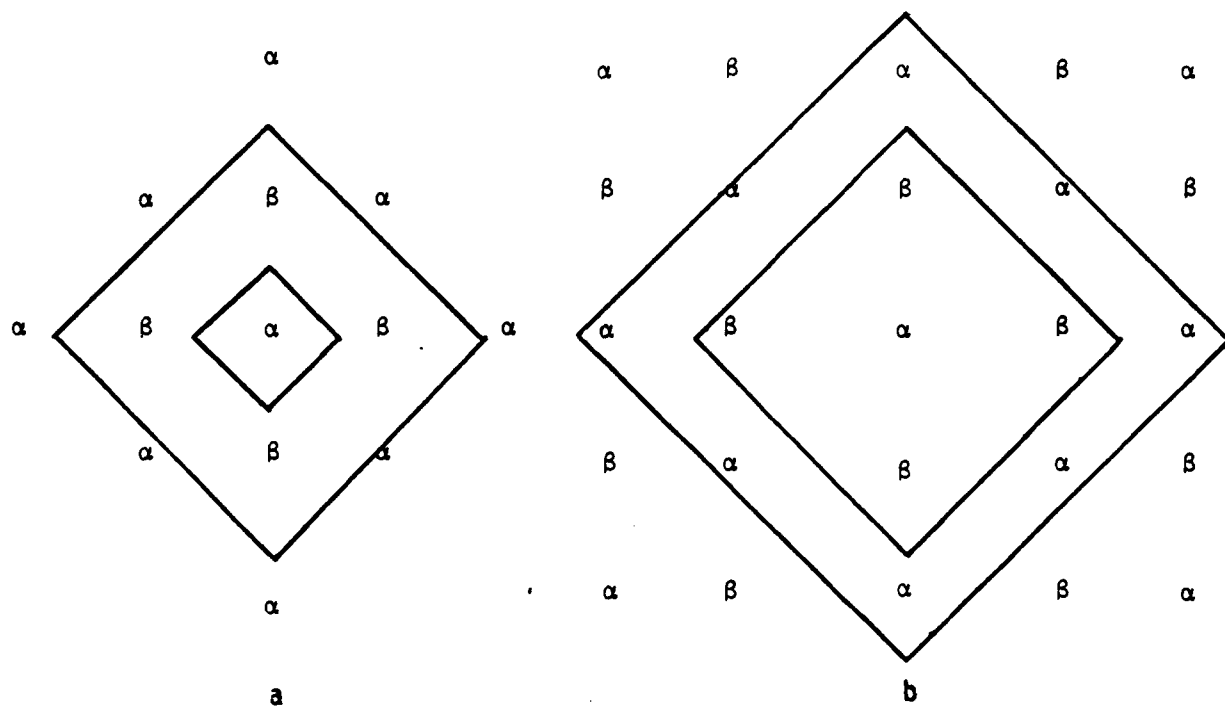


Figure 2: Lattice collection in Bethe's approximations

The group consists of an interior and a boundary, all remaining sites of the lattice are exterior. The influence of the exterior atoms are taken into account only on the average. For simplicity the method is developed for an AB alloy.

For the first approximation we select an α site as the interior. Thus the boundary will consist of z nearest neighbor β sites. For the second approximation the group may be selected as in Fig. (2b); the larger the group chosen, the greater the accuracy, however the mathematics become correspondingly more complicated [28]. Considering the first approximations, we assume that a state of long range order exists in the exterior. This ordering will affect the boundary of our group by encouraging A atoms to α sites and B atoms to β sites. This tendency to order on the boundary, due to the exterior is denoted by an ordering energy u . The energy u is equal to the difference in energy of a wrong atom on an α or β site and a right atom on an α or β site.

Consider now, the energy of the alloy which is determined by the number of pairs Q_{AA} , Q_{BB} and Q_{AB} for a definite arrangement of atoms on the lattice sites. The energy of a crystal of pure A with $F_A N$ atoms will be $-V_{AA}(\# \text{ of pairs})$ or $-\frac{z}{2} F_A N V_{AA} = -F_A Q V_{AA}$ and similarly for a crystal of B atoms only, the energy is $-F_B V_{BB} Q$. Thus the energy of the alloy, with respect to the pure crystals of its components is

$$E = -V_{AA} Q_{AA} - V_{AB} Q_{AB} - V_{BB} Q_{BB} - (-V_{AA} F_A Q - V_{BB} F_B Q). \quad (32)$$

This reduces to

$$E = \{V_{AA} + V_{BB}\} \frac{1}{2} - V_{AB} \} Q_{AB} = -V Q_{AB} \quad (33)$$

since

$$\begin{aligned} Q_{AA} &= F_A Q - Q_{AB}/2 \\ Q_{BB} &= F_B Q - Q_{AB}/2. \end{aligned} \quad (34)$$

So that the superlattice will be stable at lower temperatures V must be taken less than zero. The Boltzmann factor is then

$$e^{-V/KT} = \epsilon. \quad (35)$$

For the boundary, the relative probability of finding an A atom instead of a B atom due to the exterior is

$$e^{-u/KT} = \chi. \quad (36)$$

From the two Boltzmann factors above various probabilities in the interior and in the boundary may now be found.

If the central atom is A, a right atom, the relative probability of finding n wrong A atoms in the boundary, $P_r(n)$, is

$$P_r(n) = \binom{z}{n} \epsilon^n \chi^n. \quad (37)$$

If the center atom is a B atom the probability of finding n wrong atoms on the boundary is

$$P_W(n) = \binom{z}{n} \chi^n \epsilon^{z-n}, \quad (38)$$

since each of the $z-n$ right B atoms in the boundary has an interaction energy V with the wrong interior B atom. The binomial coefficient $\binom{z}{n}$ is the number of ways to arranging n wrong A atoms in the z boundary sites. The total relative probability for the interior atom being correct is

$$r_j = \sum_{n=0}^z P_r(n) = (1 + \epsilon\chi)^z, \quad (39)$$

and for being wrong is

$$w_j = \sum_{n=0}^z P_W(n) = (\epsilon + \chi)^z. \quad (40)$$

The normalized probabilities are then

$$r_\alpha = \frac{r_j}{r_j + w_j}, \text{ and } w_\alpha = \frac{w_j}{r_j + w_j}. \quad (41)$$

It is also necessary to calculate the relative probability of sites in the boundary being wrongly occupied. This is the average number of wrong atoms in the boundary divided by z . The relative probability of finding n wrong atoms in the boundary is $P_r(n) + P_W(n)$, the average number of wrong atoms in the boundary is calculated as follows:

$$\langle n \rangle = z w_\beta = \frac{\sum_{n=0}^z n(P_r(n) + P_W(n))}{\sum_{n=0}^z (P_r(n) + P_W(n))}, \quad (42)$$

here, w_β is the normalized probability of having a wrong atom in the boundary β sites, therefore

$$w_\beta = \frac{\frac{\epsilon\chi}{1 + \epsilon\chi} r_j + \frac{\chi}{\epsilon + \chi} w_j}{r_j + w_j}. \quad (43)$$

Now in order to determine the unknown energy u in X Bethe introduced a symmetry or consistency condition. Since there are an equivalent number of α and β sites and A and B atoms for an AB alloy at stoichiometry, the probability must be symmetric, i.e. the same probabilities hold whether an α or β site is chosen as the origin of our group. Thus,

$$w_{\alpha} = w_{\beta}, \quad (44)$$

This is called the consistency equation, putting equations (41) and (43) into the above equation the value of u at T can be found as a function of V and T ,

$$\left[\frac{x + \epsilon}{1 + x\epsilon} \right]^{z-1} = x. \quad (45)$$

The short range order σ and the configurational energy of the alloy can now be found. The number of AB pairs is $z-n$ for a right center atom, and n for a wrong center atom, therefore on the average the fraction of AB atoms in the alloy is

$$q = \frac{Q_{AB}}{Q} = \frac{\sum_{n=0}^z (z-n)P_r(n) + \sum_{n=0}^z nP_w(n)}{z(r_f + w_f)}. \quad (46)$$

For the AB alloy $q_m = 1$ and $q_r = .5$, thus, from eq. 31, $\sigma = 2q - 1$, or from equation (46),

$$\sigma = 1 - \frac{4\epsilon x}{1 + \epsilon x} \frac{1}{1 + x^z / (z-1)}. \quad (47)$$

The configurational energy is then

$$E = VQ_{AB} = -VQq = -\frac{VQ}{2} (\sigma + 1), \quad (48)$$

measured from the completely ordered alloy this energy becomes

$$E - E(0) = -\frac{VQ}{2} (1 - \sigma). \quad (49)$$

The long range order can be found by use of equations (2), (39), (40), and (41) and is

$$s = 2r_{\alpha} - 1 = \frac{(1+\epsilon\chi)^z - (\epsilon+\chi)^z}{(1+\epsilon\chi)^z + (\epsilon+\chi)^z} \quad (50)$$

Recalling that at complete disorder

$$r_{\alpha} = r_{\beta} = w_{\alpha} = w_{\beta} = 1/2$$

and using equation (45), the critical temperatures for an AB alloy is given by

$$\frac{V}{KT_c} = \ln \frac{z}{z-2} \quad [26].$$

In this form, extension to other lattices besides simple cubic AB alloys is quite laborious. However, this is equivalent to the quasichemical method of Fowler and Guggenheim [31]; and Takagi's combinatorial analysis [32] allows a simpler extension to different compositions and structure.

A comparison of the three early models can be seen in Figures 3, 4 and 5. All three of these models have neglected important physical considerations, as do the more recent models, these include: (1) interaction of atoms which are not nearest neighbors, (2) changes in cell size and lattice symmetry, and thermal expansion, (3) lattice vibrations, (4) limit of the validity of the ordering energy and finally, (5) effect of size differential in the ordering phenomena. A comparison of theory and experiment, Figures 6 and 7 shows poor quantitative agreement, qualitatively the models are essentially correct [26]. The more recent models are somewhat more quantitatively correct and will be briefly explained.

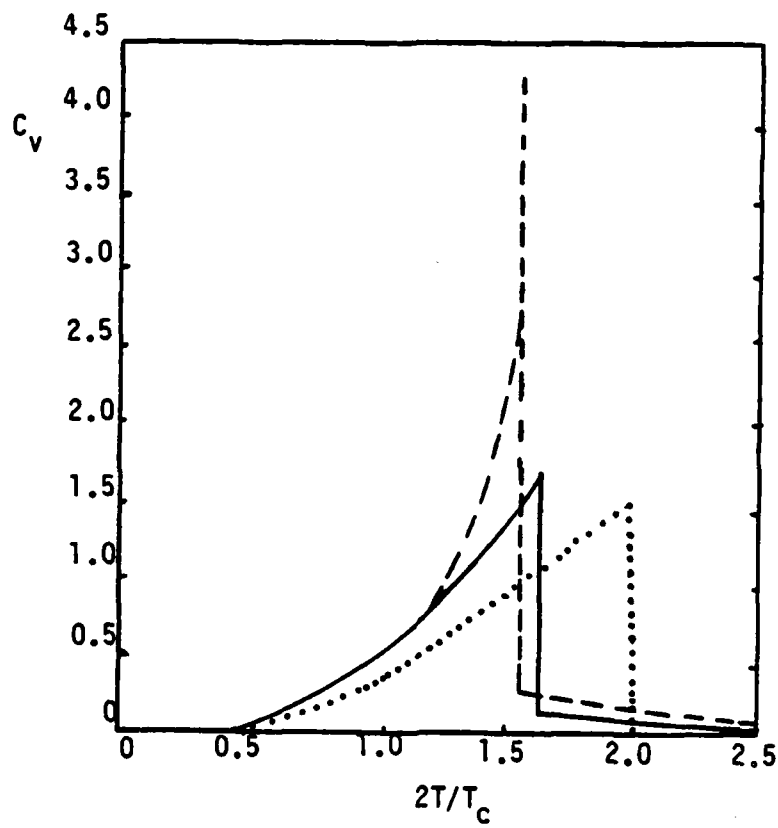


Figure 3: Configurational C_v for a simple cubic AB alloy. [26]

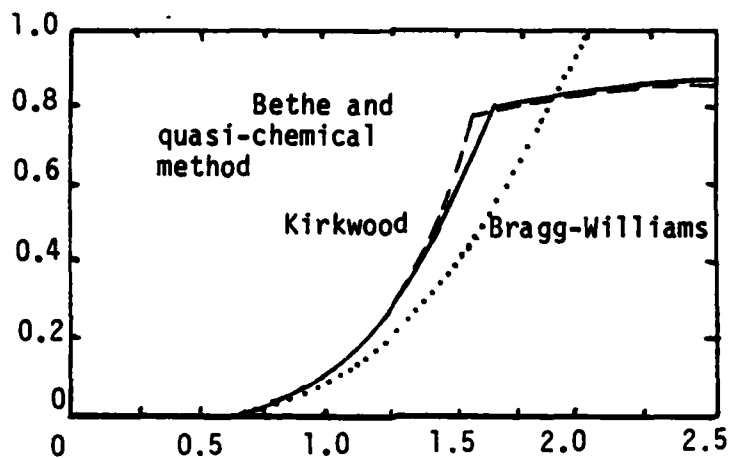


Figure 4: Configurational Energy as a function of T . [26]

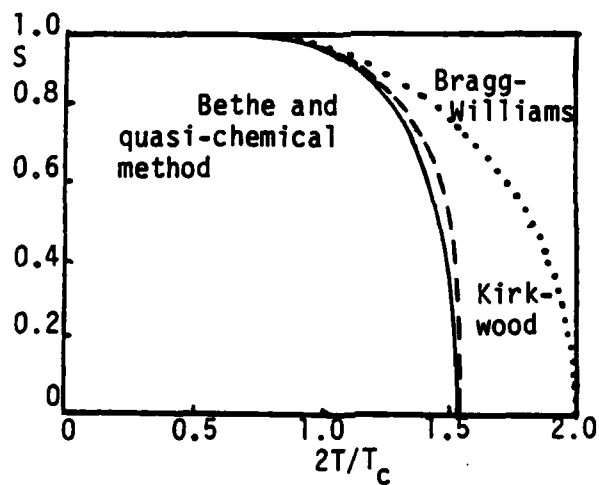


Figure 5: Long-range order S as a function of T . [26]

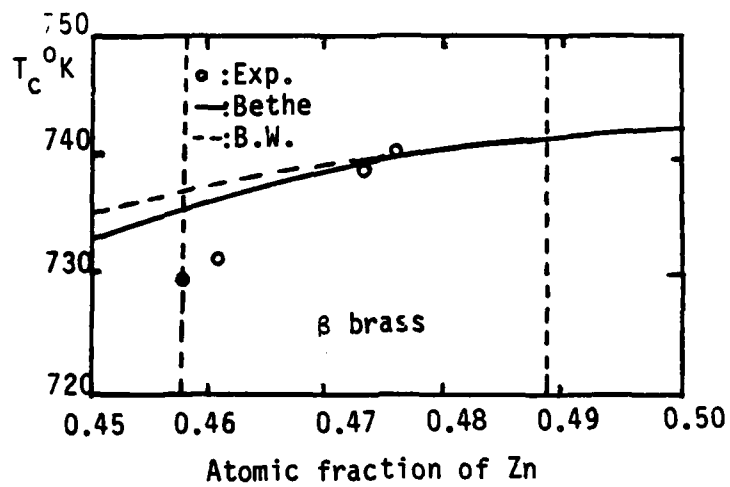


Figure 6: Comparison of T_c , Theory and Experiment. [26]

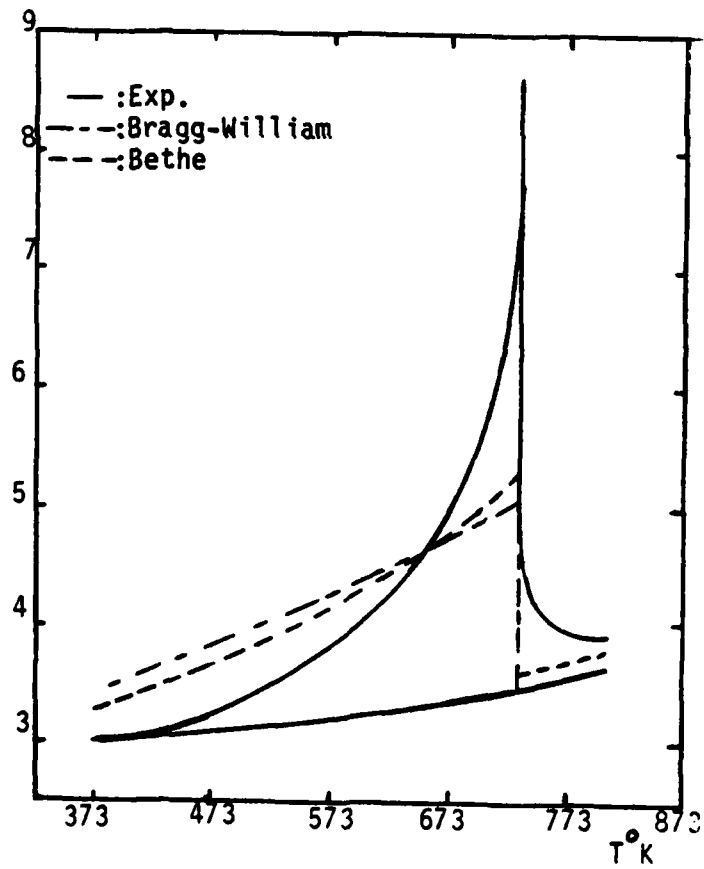


Figure 7: Comparison of Configurational C_v , Theory and experiment. [26]

iii. Cluster-Variation, Concentration Waves and Band Theory

The cluster-variation [39] method is an extension of the quasichemical model. This model uses the same type of energy terms as the earlier theories; however, it introduces a way of arriving at a better approximation to the entropy. The free energy is written in terms of the different configurations a cluster can have and is then minimized with respect to the configurations. For example, for the FCC structure a tetragonal group of atoms is chosen as the basic cluster; distribution variables are assigned to each configuration of the group and the free energy is written in terms of these variables. Minimizing the free energy with respect to these variables produces a set of simultaneous algebraic equations, usually of higher order. The values of the distribution variables which satisfy these equations represent the equilibrium configurations of the system [40]. The early formulation of the method did not allow one to choose very large clusters (which increases the accuracy) due to the large number and nature of the simultaneous equations. Kikuchi, however, has developed an iteration scheme, Natural Iteration [39], which is particularly suited to the method and guarantees convergence.

A number of authors, [41, 42, 43], have used this method and results agree fairly well with experiment and have been reproduced. This is perhaps one of the more promising methods of describing cooperative phenomena.

The idea of concentration waves was introduced by Landau [44] and Lifshitz [45] in (1937, 1941) in the development of the phenomenological theory of phase transitions of the second kind. This method, applied to the order-disorder transition in alloys [46] has proved to be fruitful. This theory enables one to understand the symmetry aspects of the order-disorder transitions, to take into consideration long range interactions in the alloy and to predict the structure of the ordered phases, which the other theories do not allow, based on concrete interatomic potentials.

All of the preceding theories reduce to the comparison of the free energy of the ordered and disordered phases calculated from nearest or at best next nearest interactions. The question of whether or not the structure of the ordered phase is stable [at the relevant choice of interatomic energies i.e. what value of i is chosen in equation (1)] and what the structure of the ordered phase is are not considered. The early theories as well as the cluster-variation improvement become especially unsatisfactory in light of recent developments in the pseudopotential theory of metal alloys and covalent compounds (a large part of the Ti-C bonds are covalent) as well as the theory of stress induced interactions in a solid solution. Studies show that interatomic interactions which are responsible for ordering cannot be short range. Thus for substantial improvement of the above theories the real long range interactions must be taken into account.

These difficulties are overcome by using the method of static concentration waves. Atomic distribution in a binary alloy can be described by means of the function $n(\bar{r})$, this one function is adequate because the occupational probabilities $n_A(\bar{r})$ and $n_B(\bar{r})$ for A and B atoms respectively are not independent, they must satisfy the identity

$$n_A(\bar{r}) + n_B(\bar{r}) \equiv 1, \quad (52)$$

here \bar{r} is a crystal lattice vector. This function can be used for interstitial as well as substitutional alloys. In the disordered state the probabilities $n(\bar{r})$ are the same for all sites which can be occupied. They are equal to the atomic fraction c of the relevant component in a substitutional alloy and in an interstitial solution they equal the fraction of interstitial sites which are occupied. In the ordered phases $n(\bar{r})$ becomes dependent on the site coordinate \bar{r} . For instance, if $n(\bar{r})$ describes t values n_1, n_2, \dots, n_t on a set

of crystal sites $\{\bar{r}\}$, then $n(\bar{r})$ describes the sublattices into which the disordered lattice has been subdivided as a result of ordering. The n_j are occupational probabilities of the sites of the 1st, 2nd -- t-th sublattice. The function $n(\bar{r})$ can be expanded in the form of a Fourier series, i.e. it can be represented as a superposition of static concentration waves:

$$n(\bar{r}) = c + \frac{1}{2} \sum_j [Q(\bar{k}_j) e^{i\bar{k}_j \bar{r}} + Q^*(\bar{k}_j) e^{-i\bar{k}_j \bar{r}}], \quad (53)$$

where $\exp(i\bar{k} \cdot \bar{r})$ is a static concentration wave, \bar{k}_j is a non-zero wave vector defined in the first Brillouin zone of the disordered alloy, \bar{r} is a site vector of the lattice $\{\bar{r}\}$ describing a position which can be occupied by an atom, the index j denotes the wave vectors in the Brillouin zone and $Q(\bar{k}_j)$ is a static concentration wave amplitude. Alternatively this can be written by combining those terms whose wave vectors \bar{k}_j 's enter into the stars (the star is a set of wave vectors \bar{k}_j , which may be obtained from one wave vector by applying to it all operations of the symmetry group of the disordered phase):

$$n(\bar{r}) = c + \sum_s n_s E_s(\bar{r}), \quad (54)$$

$$\text{where } E_s(\bar{r}) = \frac{1}{2} \sum_{j_s} [\gamma(j_s) \exp(i\bar{k}_{j_s} \bar{r}) + \gamma^*(j_s) \exp(-i\bar{k}_{j_s} \bar{r})] \quad (55)$$

$$\text{and } Q(\bar{k}_{j_s}) = n_s \gamma_s(j_s). \quad (56)$$

The summation is carried out over all wave vectors in the star, n_s are the long range order parameters and $\gamma_s(j_s)$ are coefficients which determine the symmetry of the occupation probabilities $n(\bar{r})$ with respect to rotation and reflection symmetry conditions. The requirements that in the completely ordered state, when all $n(\bar{r})$ are either zero or unity, that all n_s are equal to unity completely defines the constants $\gamma_s(j_s)$. It turns out that the concentration waves are related to the amplitude of coherent scattering in X-Ray diffraction by the equation

$$Y(q) = (f_B - f_A) \frac{1}{2} \sum_j [Q(k_j) \sum_r e^{-i(q-k_j)r} + Q^*(k_j) \sum_r e^{-i(q+k_j)r}] , \quad (57)$$

where f_A and f_B are the form factors of the A and B atoms respectively.

Now, the configuration part of the Hamiltonian of the alloy is

$$H = \frac{1}{2} \sum_{r, r'} V(\bar{r}, \bar{r}') c(\bar{r}) c(\bar{r}') , \quad (58)$$

where the summation is over all of the lattice sites and

$$c(\bar{r}) = 1 \quad \text{if there is a solute atom at } r ,$$

$$c(\bar{r}) = 0 \quad \text{if not.}$$

The interchange energy $V(\bar{r}, \bar{r}')$ is defined by the equation

$$V(\bar{r}, \bar{r}') = V_{AA}(\bar{r}, \bar{r}') + V_{BB}(\bar{r}, \bar{r}') - 2V_{AB}(\bar{r}, \bar{r}') , \quad (59)$$

This is analogous to the energy defined in equation (1), however it takes into account all interactions in the lattice.

The problem of knowing the ordered phase structure reduces to determining the function $n(\bar{r})$. Notice that $n(\bar{r})$ follows a sort of Pauli exclusion principle: each lattice site is either occupied by one or zero atoms of some definite type. Thus we can reason that it follows the Fermi-Dirac distribution:

$$n(\bar{r}) = \frac{1}{\exp \frac{-\mu + \phi(\bar{r})}{KT} + 1} , \quad (60)$$

where the chemical potential μ is determined by the condition of conservation of mass

$$\sum_r n(\bar{r}) = \sum_r \left[\frac{1}{\exp \frac{-\mu + \phi(\bar{r})}{KT} + 1} \right] = N_1 \quad (61)$$

where N_1 is the number of solute atoms. In the self-consistent field approximation, $\phi(\bar{r})$ is

$$\phi(\bar{r}) = \sum V(\bar{r}, \bar{r}') n(\bar{r}'). \quad (62)$$

This approximation neglects correlation effects.

Substituting this potential into (60)

$$n(\bar{r}) = \frac{1}{\exp \frac{-\mu}{KT} + \frac{1}{KT} \sum V(\bar{r}, \bar{r}') n(\bar{r}') + 1}, \quad (63)$$

which corresponds to the free energy

$$\Omega = U - TS - \frac{\mu \sum n(\bar{r})}{r}, \quad (64)$$

where $U = \frac{1}{2} \sum_{\bar{r}, \bar{r}'} V(\bar{r}, \bar{r}') n(\bar{r}) n(\bar{r}')$

is the internal energy and

$$S = -k \sum_{\bar{r}} [n(\bar{r}) \ln(n(\bar{r})) + (1 - n(\bar{r})) \ln(1 - n(\bar{r}))] \quad (65)$$

is the entropy. The Helmholtz free energy of the system is

$$F = U - TS. \quad (66)$$

By using the expression for $n(\bar{r})$ in equation (54), and equation (63) the equilibrium values of n_s at T can be found:

$$c + \sum_s n_s E_s(\bar{r}) = \exp \frac{-\mu + V(0)c + \sum_{s=1}^{t-1} V(\bar{k}_s) n_s E_s(\bar{r})}{KT} + 1. \quad (67)$$

Here $V(\bar{k}) = \sum V(\bar{r}) e^{i\bar{k}\bar{r}}$ is the Fourier transform of the interatomic potential, and can be found by measuring the diffuse scattering intensity from a single crystal of the disordered alloy, [46]

$$I_{diff}(\bar{k}) = (f_A - f_B)^2 \frac{c(1-c)}{1 + \frac{c(1-c)}{kT} V(\bar{k})}. \quad (68)$$

This method can predict the critical temperature, ordered structure and stability apparently with much more ease and accuracy than the former theories [46]. The critical temperature calculated for the CuAu₃ alloy by this method is only 19° lower than the actual experimental value. This accuracy is exceptional as compared to the previous models; it also has the advantage that the interaction energies are in no way ambiguous and are measurable through X-Ray diffraction.

One of the band theory models of the ordering phenomena [37] uses a tight binding Hartree Hamiltonian to determine the ordering energy incorporated with the cluster-variation method for the entropy of the system. Here the bulk density of states is derived from a configurational average over the local densities of states at the central site of a cluster. The free energy of the alloy is determined by minimizing a model free-energy function over the space of possible electron-ion configurations. These configurations may be classified by the values of certain order parameters $\{\alpha_l\}$ which measure multi-site correlations, e.g., long-range order, short range order, three-body correlations, etc. Thus at a temperature T,

$$\begin{aligned} F(T,c) &= \min_{\alpha_l} F(T,c;\alpha_l) \\ &= E(T,c;\alpha_l) - TS(c,\alpha_l) \end{aligned} \tag{69}$$

where c is the composition. A schematic of the free energy calculation is shown in Figure 8.

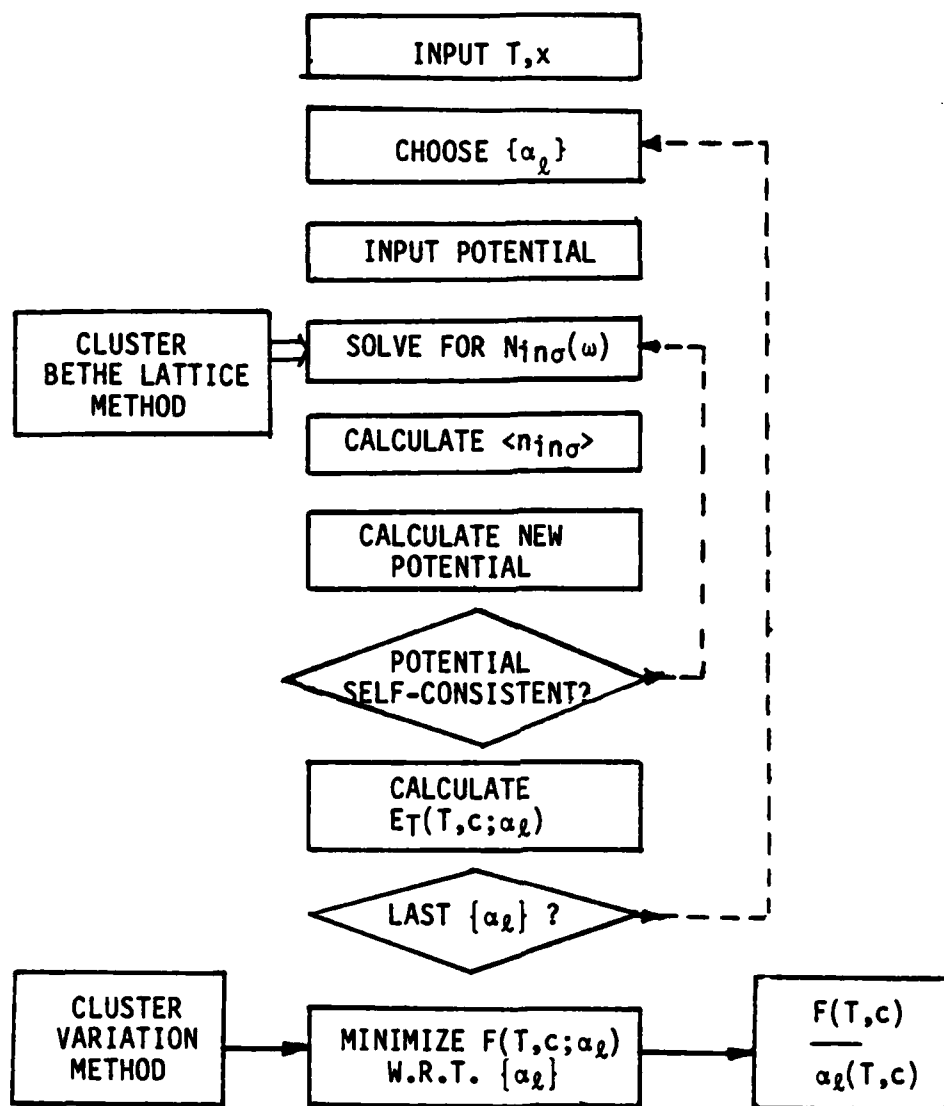


Figure 8. Block diagram showing basic steps to self consistent electronic theory of the alloy ordering energy and in determining alloy thermodynamics. [37]

In Figure 8., $N_{i n \sigma}(w)$ is the local density of states and $\langle n_{i n \sigma} \rangle$ is the thermal averaged occupation of sites.

This model predicts a critical temperature of the CuAu system which is in error by 19% which is more accurate than the early set of models but can not compare with the accuracy obtained in the method of concentration waves. One notable point of this theory however is that it actually calculates the atomic interaction energies as a function of short-range order, these energies are constant only near $\sigma=0$ and can vary in magnitude as much as 60%. This makes the early Ising models and the cluster-variation model even more unsatisfactory since they are based on an a priori knowledge of this energy, which is assumed constant at all values of order.

Since Fosdick [38] first applied the Monte Carlo Method to order-disorder transformations in solids a number of attempts have been made to improve and extend this procedure [47]. Unfortunately the stability of any given configuration in this model is again based on the nearest neighbor interaction energies. Since the method can require quite a lot of computation time and exhibits the same energetic restrictions as early Ising theories this method of approaching the problem of ordering does not seem to be worth the efforts in our present research effort.

iv. Ordering Energy

It seems that the most productive model available to the predictions of the ordering phenomena lies in the method of static concentration waves and this is probably the theory which we will use in predicting the ordering properties of the Ti-C system. The absence of ambiguity as far as energy terms are concerned makes this theory much more desirable than the Ising models. The band model is orders of magnitude more involved, as well as less accurate. However, it will be desirable to compare predictions made by the Ising models and to this end an understanding of the ordering energy in equation (1) is necessary.

Some justification of choosing nearest neighbor interaction energies instead of long-range effects in ordering seems to be found in the quantum theory which holds that forces between atoms decrease rapidly as the distance separating them increases. As stated earlier, the pair interaction energies V_{AA} , V_{BB} are the interaction energies between pairs of atoms in the pure elemental crystals and V_{AB} the interaction in the alloy. However, this definition is very ambiguous. What do we measure to find these energies, or how do we calculate them? The energy V^1 in equation (1) is the first term in the expansion of the Fourier Transform of the long-range interaction energy used in the static concentration wave model, where for a FCC lattice, [46]

$$V(K_0) = V(2\pi a^*z) = -4w_1 + 6w_2 - 8w_3 - \dots \quad (70)$$

where w_i are the energies corresponding to each coordination shell.

The simple nearest neighbor approximation has been shown to be extremely crude [49,50], for instance, it cannot explain why most order-disorder transformations are first order, why the maximum value of T_c often occurs away from stoichiometry or why an FCC alloy should order at all. Freidel [50] and others [51] have been able to show that because conduction electrons in a

metal are limited to energies below the Fermi surface a complete screening of the ionic metal cores are not possible, thus long range effects are present. The pseudo-potential theory [52] also points to many body interactions. However, neither one of these methods of calculating interaction energies can be used for the alloy system under investigation with any faith due to the presence of covalent bonding. These bonds have a strong angular nature and many body interactions [23].

A theory recently developed to find the ordering energies of transition metal alloys [53] is available, however it has not been used and requires quite a few parameters which might be as difficult as the ordering energies themselves to obtain.

In addition to the extensive literature search for methods to calculate and measure the ordering energies we also consulted several members of the faculty in chemistry and solid state physics here at Auburn about this problem and without exception they all suggested using heats of formations for these energies. After looking in several references [54,55] we found values that were experimentally verified (see table 1) and used these in calculating the critical temperature for the Cu-Au alloy system.

bond	energy
Au-Au	88 \pm 0.5 kcal/mole
Cu-Cu	80.7 kcal/mole
Au-Cu	55.4 \pm 2.2 kcal/mole

Table 1. Heats of formation of standard states from monatomic gases.

The critical temperature calculated from these values using the Bragg-Williams approximation was five orders of magnitude higher than the measured value. Clearly the heats of formation are not the interaction energies which we are

looking for, although they must be connected in some way. The literature had nothing to say on this connection however and the idea of using the heats of formation for ordering energies has been abandoned. It now appears that the only way to arrive at an acceptable number for these energies is through X-Ray diffraction.

v. Summary

Although there have been quite a number of theories put forth since the pioneer work of Bragg-Williams, most of them seem to exhibit the same shortcomings (though perhaps not as severe) as this first approximation. It seems however, that the use of the method of static concentration waves, coupled with X-Ray diffraction experiments will give satisfactory results. It has been somewhat distressing to find after a very extensive literature search, (both with a computer and in the library) that very little work has been done in actually finding, theoretically or experimentally, the needed interaction energies. Although there is one theory available to calculate the ordering energies [53], no one has used it and it is doubtful that we will be able to due to its complexity. Clapp and Moss have done some diffraction work in the Cu-Au system in which they have tried to find the pair-wise interaction energies, however, basically what they have done is fit this to the known critical temperatures [57]. Semenouskaya [58] using X-Ray work done by Moss [59] has attained remarkable results in calculating the ordering temperature of Cu_3Au as stated before and it is hoped that we will be able to employ this same method and attain the same kind of results. The measurements made were the absolute intensity of X-Ray diffuse scattering by the disordered alloy. There are a few references in the literature on diffraction studies done with single crystal Ti-C, however we will undoubtedly require more data than is available. To this end we will have to take diffraction patterns with powdered samples.

Now that the literature search and study is nearing completion the main problem to be tackled at this time is the calculation or measurement of ordering energies so that predictions of the critical temperatures, etc. can

be made. To this end powder samples from the alloys already melted will be made and an analysis of the diffuse scattering of X-Rays from the samples carried out. From the intensities, it is hoped that an accurate measurement of the ordering energies will be possible. The effort to theoretically come by these energies will also continue. Once these energies are found the ordering properties of the alloy system will be studied at various compositions and the most promising of these compositions will be concentrated on in the experimental phase.

Besides predicting the structure and ordering temperature of the alloys, compression tests at elevated temperatures are planned, as well as measurements of the specific heats. Once the properties of these alloys are well understood, additional elements may be alloyed with the Ti-C to improve any undesirable properties such as brittleness.

Efforts to determine the effects of additional alloying elements will be made after Kikuchi [24]. These calculations in conjunction with electron density calculations will point to the best choice of alloy additives. These studies will form a strong basis for the additional study and optimization of the alloy system.

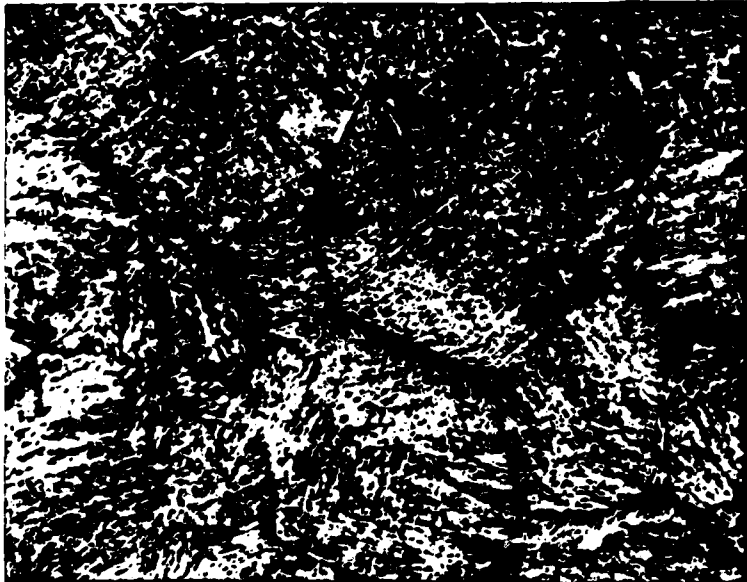
B. Experimental Progress

The C-Ti system was identified as the most promising alloy system based upon the ability to obtain an ordered structure over a range of compositions and the ultrahigh melting temperature of the system (melting point of 3080 C). A series of C-Ti alloys was melted to investigate the properties of the system. Fifteen compositions were melted covering the range 0 to 22 weight percent carbon. The initial alloy melts did not include additions for improvement of ductility to enable a direct comparison between theoretical predictions of ordering parameters and experiment. Initial melts were made by arc melting under an Argon cover gas.

The arc melting unit used to produce the initial C-Ti melts consists of a gas cooled electrode (0.38 inch diameter stinger) which is composed of Tungsten-2% Thoria and a graphite crucible approximately .5 inches in diameter by .25 inches high. To produce these melts, direct current voltages of 35-40 volts and 450-575 amps were required. Some problems were encountered during the arc melting process because of the high melting temperatures needed to produce the alloys. An inert gas flow rate that was higher than normal was necessary to keep the Tungsten stinger from melting. This inert gas flow had a tendency to blow the carbon additions out of the crucible, resulting in some of the melts having a carbon composition less than desired. Compositions of the alloys have not been checked and hence reported compositions are nominal compositions which do not reflect such losses. Samples produced by this method were restricted to buttons less than 5 cubic centimeters in volume. For melts larger than this it was impossible to keep the entire specimen molten throughout the procedure.

Figures 9 through 12 show representative microstructures of the fifteen alloys produced by this arc melting procedure. Figure 9 is the photomicrograph of a 1 weight per cent (w/o) carbon-titanium alloy which was generated by the arc melting procedure in a carbon crucible. Figures 10 through 12 are microstructures of alloys with increasing carbon content. The figures show that the microstructures that one obtains become more complex as carbon content is increased. In the low carbon alloy (Figure 9) the microstructure is dominated by a single phase with carbide particles distributed along the grain boundaries. However the 22 weight percent carbon alloy structure (Figure 12) consists of at least four distinct phases. Different structure morphologies were also identified from the optical micrographs. The microstructure of Figure 10 (a 12 w/o carbon alloy) is dominated by a dendritic structure while the microstructure of Figure 11 (a 16 w/o carbon alloy is dominated by a Widmannstätten pattern.

Figure 13 is the phase diagram for the C-Ti system. Comparing the results with published phase diagrams for the C-Ti system one finds good agreement between the anticipated phases and the microstructure for alloys of 12 w/o carbon and below. It should be pointed out that the phase diagram of this system has not been extensively investigated. For carbon concentrations greater than 12 w/o and temperatures above 1500°C, the diagram is based on theoretical calculations. For compositions with carbon content less than 12 w/o, the structure should consist of a mixture of α -Ti and γ phases. This is what was obtained in the alloys shown in Figure 9 (1 w/o carbon) and Figure 10 (12 w/o carbon). However for alloys with carbon concentrations above 12 w/o, more than two phases were found in the microstructures. According to the phase diagram, the phases present should be α or γ +graphite. One of the phases in Figure 11 and Figure 12 is graphite, but there appears to be at least



400 μm

Figure 9: Ti plus 1 w/o Carbon Alloy. Structure consists of α -Ti phase with TiC carbides at grain boundaries.



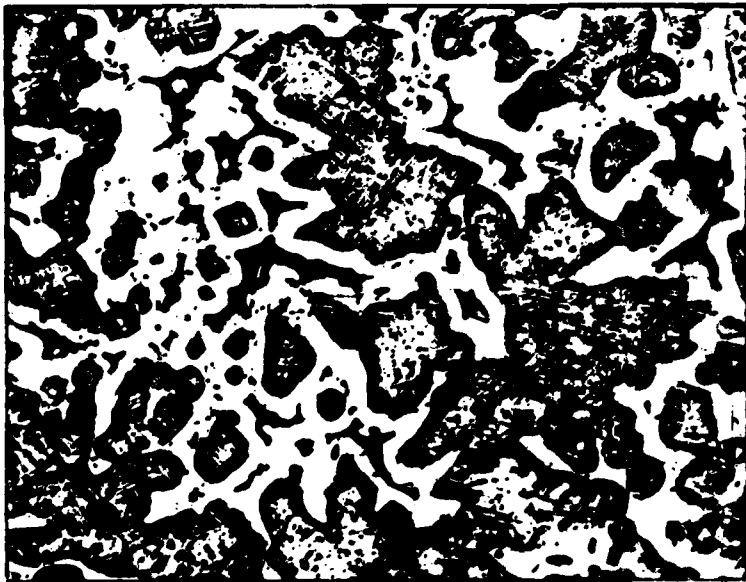
100 μm

Figure 10: Ti plus 12 w/o Carbon Alloy. The alloy structure consists of γ matrix with α -Ti phase dendrites.

two other phases which do not appear on the phase diagram. X-ray diffraction studies are being performed in an attempt to identify the phases present in the alloys of Figure 10 and 12, as well as the degree of order achieved in the γ phase.

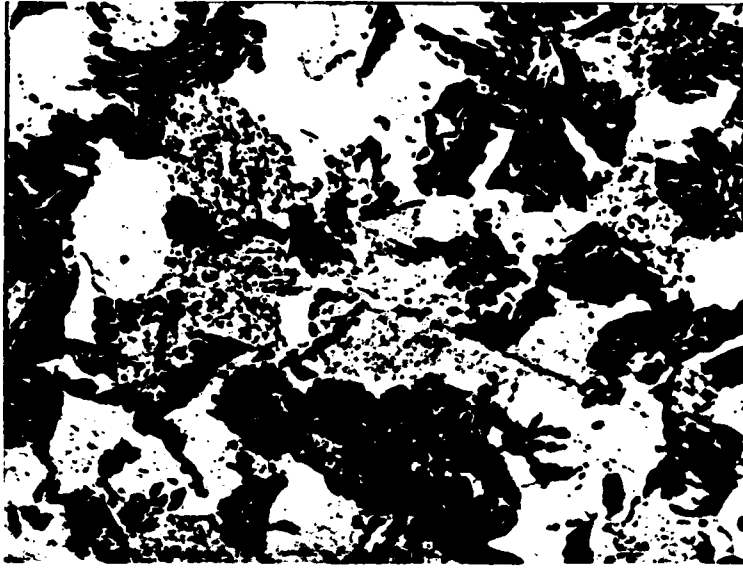
Hardness measurements were made on the alloys to scope the mechanical properties. The macroscopic hardness measurements were found to be relatively insensitive to carbon content. The Rockwell C hardness varied from a value of 20 for the 1 w/o carbon alloy to 52 for the 22 w/o carbon alloy. The high carbon alloys were found to crack if the hardness indentation was applied near the edge of the test specimen. In addition to macrohardness measurements, an attempt to make microhardness measurements on the various phase structures seen in Figures 9 through 12 was made. This attempt was only partially successful. Only on the α -Ti phase could valid readings be obtained. Attempts to make indentations on other phase structures were unsuccessful. No detectable indentations occurred for the applied loads. It has been hypothesized that the other phases have a hardness greater than DPH 2000 which is the upper limit of our microhardness test machine at the present time. A special weight pan is being purchased to increase the load that can be applied to the specimen and microhardness tests will again be made.

Recently a new induction heating system was delivered to Auburn which was purchased under this contract. It consists of a 5 kilowatt generator with induction coil to which a quartz tube for maintaining an inert gas atmosphere has been attached. About a month of effort was spent tuning the frequency of the induction generator and experimenting with coil design to obtain the higher temperatures required in melting and sintering the carbon-titanium alloys. The coil shape and diameter of the spiral controls the concentration



100 μm

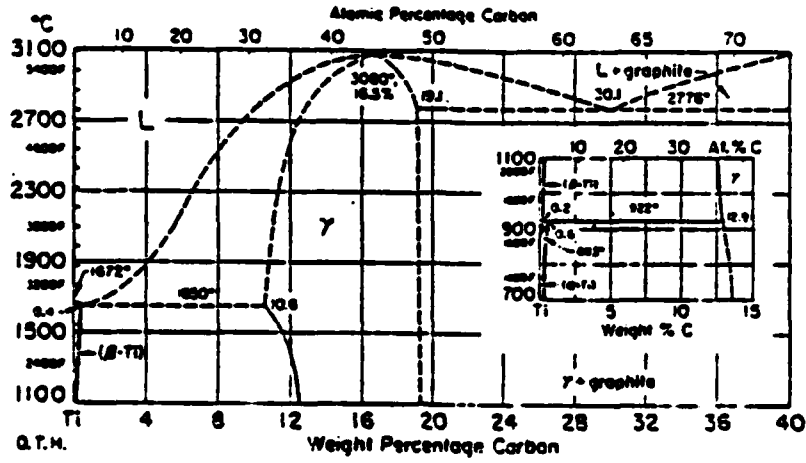
Figure 11: Ti plus w/o carbon alloy. The alloy structure consists of the α -Ti phase plus γ phase and free graphite.



200 μm

Figure 12: Ti plus 20 w/o carbon alloy. The alloy structure consists of free graphite and γ phase. Two additional phases appear to be present which do not appear on the equilibrium phase diagram.

C-Ti Carbon-Titanium



from reference 22

Figure 13: Phase diagram for the C-Ti alloy system. Note that the dashed lines indicate calculated phase relations.

of energy on the melting volume. The frequency of the induction generator can be varied to induce deep penetration or surface heating of the material or maximize the heating effect as a function of alloy system. Although higher melting temperatures are obtained as the diameter of coil spiral is decreased, the size of the melt and the fabrication of the coil becomes more difficult. The diameter of the copper tube is fixed in the present system in order to maintain adequate cooling of the induction coil. A photograph of this system in operation is shown in figure 14.

With this simple system an additional ten melts have been made of carbon-titanium alloys covering the range 0-14 weight per cent carbon. Although there are still problems with obtaining a homogeneous material composition and eliminating porosity of the melt, alloys produced using this system are greatly improved over those produced by previous methods. We continue to experience difficulty in obtaining a fluid mixture of the alloy for carbon compositions above 10 w/o. Sintering of the carbon and titanium is obtained but there is no real melting. From these newly produced alloys two compression samples were cut for mechanical properties testing. The carbon content of these titanium alloys were 4 w/o and 5 w/o carbon. Macrohardness tests were conducted on the alloys yielding a value between 30 and 40 Rockwell C.

A diamond slitting saw was used to prepare cube compression specimens because of the small size of the available material. Although the alloys were not excessively hard, large amounts of time were required to prepare the compression samples which measured 2.29mm X 2.29mm X 12.7mm high. The alloys were gummy in nature requiring sharpening of the diamond blade with a carbon

block to remove cut particles stuck in the blade. Compression tests were conducted at room temperature using a Materials Testing System. The data were simultaneously recorded on a HP X-Y chart recorder and through a digital HP 9836 data acquisition system. Figure 15 is the stress-strain curve for the compression test of the 5 w/o carbon sample.

A summary of the mechanical properties of the two titanium-carbon alloys along with properties for pure titanium and Ti-6Al-4V alloys is given in Table 2. The pure Ti and Ti-6Al-4V data was taken from the ASM Metals Handbook [60] and is based on tensile specimens. Both of the compression samples showed visible signs of porosity on the surface prior to testing (Figure 16). Despite the observable flaws in the specimens, exceptional yield, ultimate and elongation values were obtained for the 5 w/o carbon alloy. A yield strength of 100 ksi, UTS of 164 ksi and elongation of 5.4% is very impressive when compared to a 120 ksi yield strength, UTS of 130 ksi and 4% elongation of forged Ti-6Al-4V. In addition the melting temperature of the 5 w/o carbon alloy is expected to be 2000°C compared to the melting point of Ti-6Al-4V of 1650°C.

Both compression samples failed on a plane of approximately 45 degrees to the tensile axis along a line connecting several of the pores on the specimen's surface. The 4 w/o carbon specimen failed prematurely due to an interior gas pocket which was visible after the test. Optical photomicrographs of the two structures are given in figures 17 and 18. Two separate distinct phases appear which is consistent with the phase diagram. The properties of the alloys appear to be reversed, however, the 5 w/o C alloy is less hard than the 4 w/o alloy. Verification of the alloy composition needs to be confirmed prior to any conclusions being drawn as to the effect of increasing carbon content on the mechanical properties.

Table I

Summary of Mechanical Properties

<u>Alloy</u>	<u>Melting Temp(°C)</u>	<u>Yield (Ksi)</u>	<u>UTS (Ksi)</u>	<u>Elongation (Ksi)</u>	<u>Modulus (10⁶psi)</u>	<u>Hardness</u>
Ti-4C	1900	42.4	54.2	1.4%	12.8	41R _C
Ti-5C	2000	100	164	5.4%	30.8	32R _C
Ti	1665	20.3	34.1	54%	16.8	70 HB
Ti-6Al-4V	1650	120	130	4.0%	15.4	32R _C



Fig. 14 Induction generator and melting furnace used to produce Ti-C alloys for compression testing

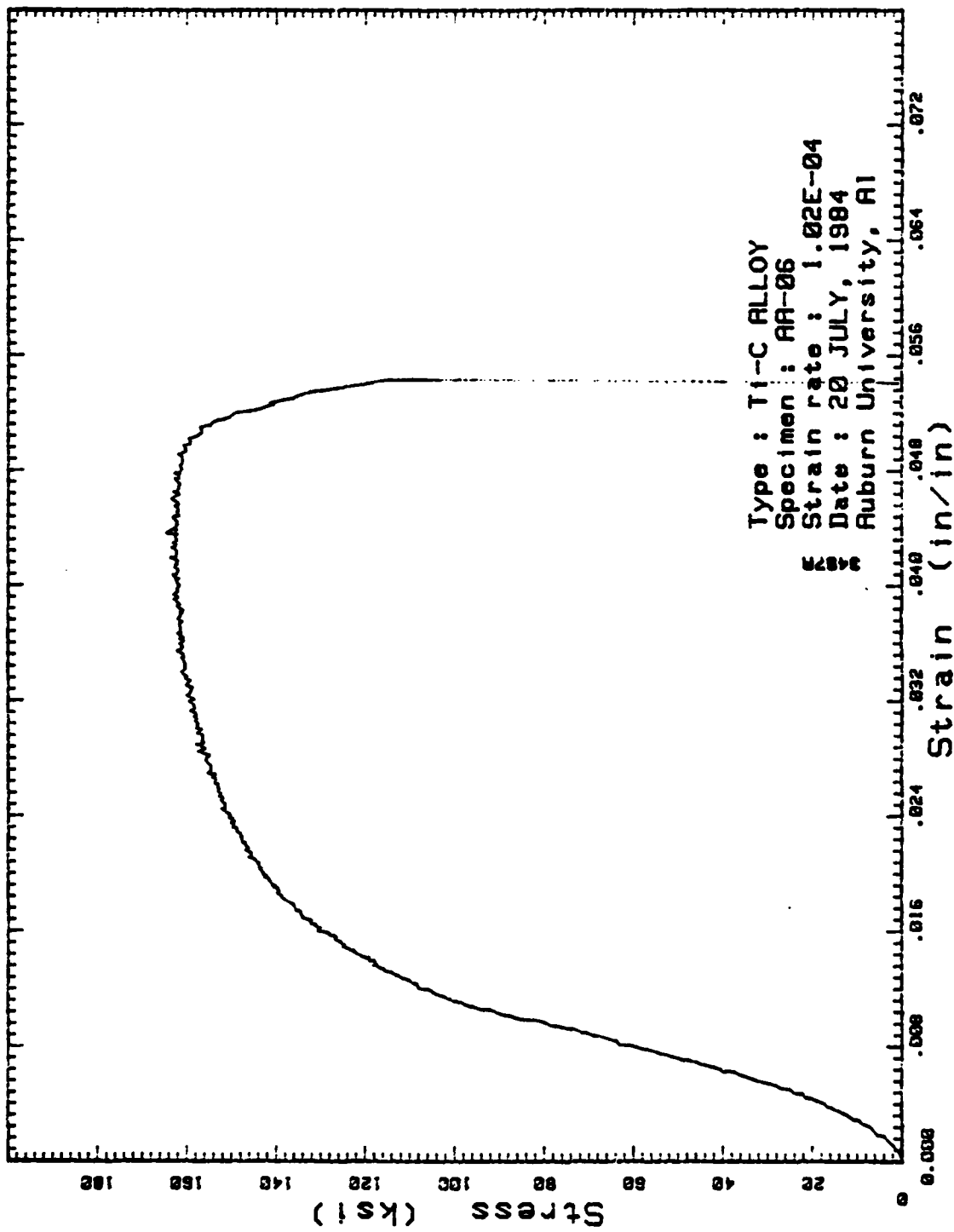


Figure 15: Compression Stress-strain curve for Ti-5 w/o carbon alloy

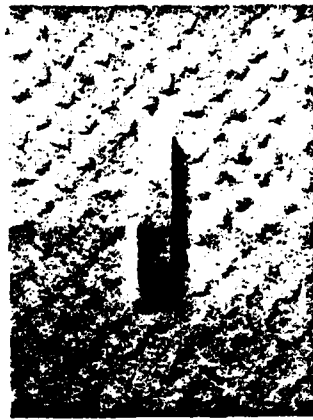
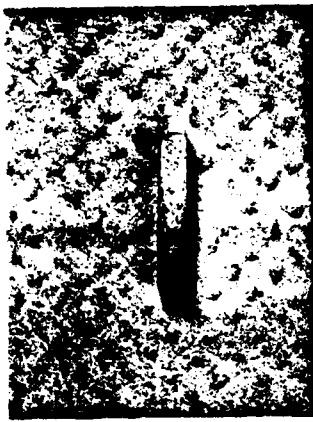


Figure 16: Compression Test Samples 4 w/o C and 5 w/o C. Note small amounts of porosity on surface.

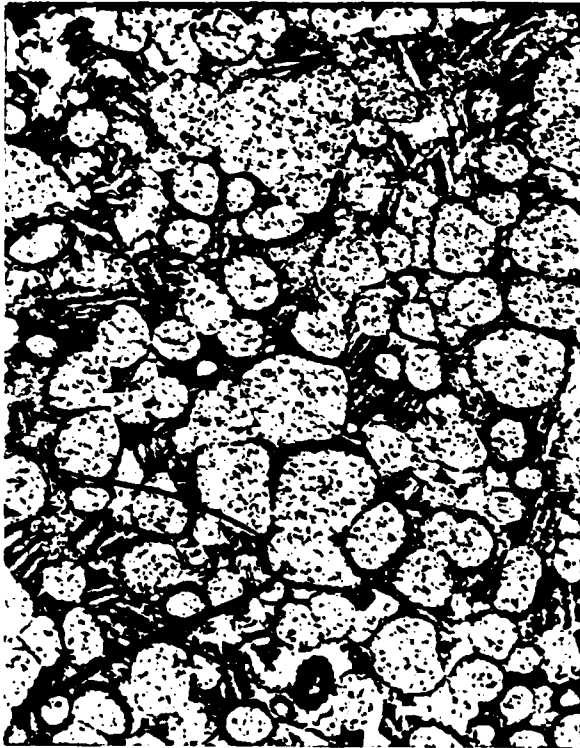


Figure 17:

Transverse photomicrograph of Ti-4 w/o C Alloy. Globular phase is α -Ti. Volume fraction of α -Ti is 62%.

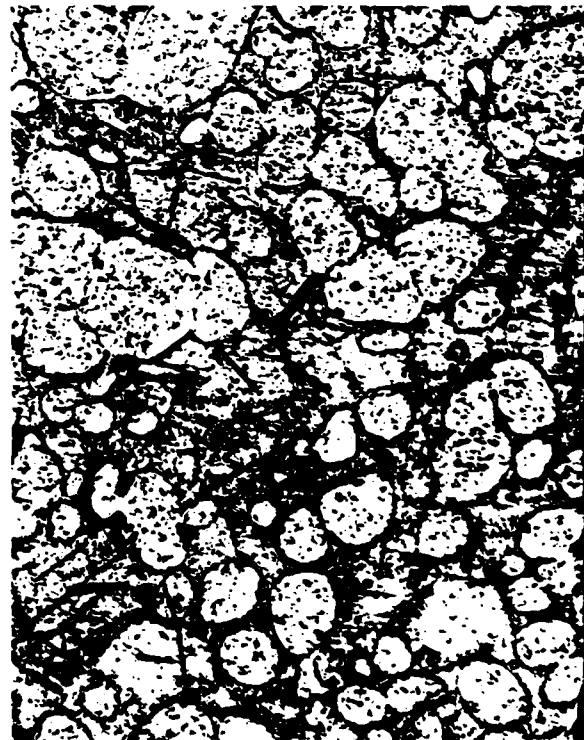


Figure 18:

Transverse photomicrograph of Ti-5 w/o C Alloy. Volume fraction of α -Ti is 54%.

Based upon our initial experience with the melting of the C-Ti alloys, two of the principle areas which must be improved are grain boundary structure and uniformity of composition throughout the melt. In alloys with carbon additions greater than 12 w/o, the graphite is found to reside along the grain boundaries or as blocky phases in the matrix. A more uniform distribution of constituents is anticipated to improve the ductility and also enhance the strength. An additional improvement which is being pursued is the elimination of grain boundary impurity elements such as the halide elements which are naturally attracted to the grain boundaries. An ultrahigh vacuum furnace capable of 2700°C is being assembled for melting and heat treatment of the second generation of C-Ti alloys. The future melts of C-Ti alloys will contain between 1 and 5 w/o Nb and 0.5 w/o Ce to improve the matrix ductility through control of the e/a ratio and reduce the segregation of impurity elements at the grain boundaries.

V. CONCLUSIONS

- A theoretical study to predict critical ordering temperatures and compositions in ordered alloys has been initiated. Scoping calculations have identified the C-Ti system as the most promising system in which the ultra-high strength, ductility and temperature resistance can be obtained.
- A total of twenty-five Ti-C alloys have been manufactured covering compositions of 0-22 w/o C. Optical metallography on specimens with greater than 12 w/o seem to show phases which do not appear on standard phase diagrams of the C-Ti system.
- Compression tests on a 5 w/o C sample at room temperature show a yield stress of 100 ksi, ultimate tensile strength of 164 ksi and strain to fracture of 5.4%. These properties are better than forged bar Ti-6Al-4V properties.

VI. REFERENCES:

1. F. J. Homan, "Fueled Graphite Development", Gas Cooled Reactor Programs, Annual Progress Report, ORNL-5753. August 1981, pg 19.
2. N. S. Stoloff and R. G. David, "The Mechanical Properties of Ordered Alloys, Progress in Materials Science, Vol. 13, (1), 1966, p 1.
3. B. H. Kear, C. F. Sims, N. S. Stoloff and J. H. Westbrook, Eds., Ordered Alloys Structure and Physical Metallurgy, Proc. 3rd., Bolton Landing Conf., Lake George, N.Y., Claiter's Pub. Div. (1970).
4. M. A. Krivoglaz and A. A. Smirnov, The Theory of Order-Disorder in Alloys, American Elsevier Pub. Co., New York (1964).
5. F. Muto and Y. Takagi, The Theory of Order-Disorder Transformations in Alloys, Academic Press, New York (1956).
6. L. E. Popov and N. A. Koneva, Order Disorder Transformations in Alloys, J. Warlimont, Ed., Springer-Verlag, New York (1974), p 404.
7. M. J. Marcinkowski, Order Disorder Transformations in Alloys, J. Warlimont, Ed., Springer-Verlag, New York (1974), p 364.
8. A. E. Vidoz, D. P. Lazarenio and R. W. Chan, Acta Met, Vol. 11 (1963), p. 17.
9. B. H. Kear and H. Wilsdorf, Trans AIME, Vol. 224 (1962), p 382.
10. R. C. Boetlner, N. S. Stoloff and R. G. Davis, Trans AIME, Vol. 236 (1966), p 131.
11. E. M. Schulson, "Order Strengthening as a Method for Reducing Irradiation Creep: An Hypothesis", Journal of Nuclear Materials, Vol. 66, (1977), p. 322.
12. C. T. Liu, "Development of Iron-Base Alloys with Long Range Ordered Crystal Structure", ADIP Quarterly Progress Report, DOE/ER-0045/1, April, (1980), p 72.
13. D. N. Braski, "Resistance of (Fe, Ni) V Long Range Ordered Alloys to Radiation Damage", Alloy Development for Irradiation Performance, Proceedings of DOE Program Review Meeting, Sept. 30 - Oct. 1, (1980), p. 367.
14. R. W. Carpenter and E. A. Kenik, "Stability of Chemical Order in NiMo Alloy Under Fast Electron Irradiation", in Proceedings of 35th Electron Microscopy Society, Claitor's Publishing, Baton Rouge, LA, 1977.
15. G. J. E. Carpenter and E. M. Schulson, J. Nuclear Materials, Vol. 23, (1978), p. 180.

16. E. M. Schulson, J. Nuclear Material, Vol. 56, (1975), p. 38.
17. E. M. Schulson and M. H. Stewart, Met Trans B., Vol. 78, (1976), p. 363.
18. L. E. Tanner, P. Stark, E. T. Petters, J. J. Ryan, I. Vilks, and S. V. Radcliffe, AST-TDR62-1087 Man Labs Inc., Cambridge, MA, 1963.
19. D. T. Liu, "Development of Long Range Ordered Alloys", Alloy Development for Irradiation Performance, Proceedings of Program Review Meeting, Sept. 30 - Oct. 1, 1980, p 354.
20. C. T. Liu and H. Imouye, "Control of Ordered Structure and Ductility of (Fe, Co, Ni)₃ V Alloys", Met. Trans A., Vol. 10, (1979), p. 1515.
21. C. T. Liu, "Development of Alloys with Long Range Order", ADIP Quarterly Progress Report, DOE/ET-0058/1, Aug. 1978.
22. M. Hansen, Constitution of Binary Alloys, McGraw-Hill, New York, (1958), p. 370.
23. T. Lyman, ed., "Metallography, Structures and Phase Diagrams", Metals Handbook, Vol. 8, (1973), p. 279.
24. R. Kikuchi, Acta Metall. Vol. 25, (1977) p. 195
25. G. Tammann, Z. anorg. Chem. (1919) p. 107
26. T. Muto and Y. Takagi, The Theory of Order-Disorder Transitions in Alloys, Academic Press, New York, Solid State Reprints. (1955)
27. W. L. Bragg, and E. J. Williams, Proc. Roy. Soc. Vol. A145, (1934); p. 699; Vol. A151, (1935); p. 540; E. J. Williams, Proc. Roy. Soc., Vol. A152, (1935), p. 231
28. H. Bethe, Proc. Roy. Soc. Vol. A150, (1935), p. 552.
29. J. G. Kirkwood, J. Chem. Phys. Vol. 6, (1938) p. 70.
30. E. A. Guggenheim, Proc. Roy. Soc. Vol. A148, (1935), p. 304.
31. R. H. Fowler and E. A. Guggenheim, Proc. Roy. Soc., Vol. A174, (1940), p. 189, E. A. Guggenheim, Proc. Roy. Soc. Vol. A184, (1944), p. 221.
32. Y. Takagi, Proc. Phys-Math., Soc. Japan, Vol. 23, (1941), p. 44.
33. R. Kikuchi, Phys. Rev., Vol. 81, (1951), p. 988.
34. C. N. Yang, J. Chem. Phys. Vol. 13, (1945); p. 66; C. N. Yang and Y. Y. Li, Chinese Phys. Vol. 7, (1947); p. 59; Y. Y. Li, J. Chem. Phys., Vol. 17, (1949). p. 447.
35. T. L. Hill, J. Chem. Phys. Vol. 18, (1950), p. 988.

36. A. G. Khachaturyam, *Physics Metals Mettlog.* Vol. 13, (1962) p. 493; *Sov. Phys. Solids St.* Vol. 5, (1963) p. 16; *Sov. Phys. Solid St.*, Vol. 5, (1963), p. 548.
37. R. C. Kittler and L. M. Falicov, *Phys. Rev. B*, Vol. 18, (1978) p. 2506.
38. L. D. Fosdick, *Phys, Rev.* Vol. 116, (1959) p. 565.
39. R. Kikuchi, *J. of Chem. Phys*, Vol. 60, (1974) p. 1071.
40. M. Kurata and R. Kikuchi, *J. Chem. Phys.*, Vol. 21, (1953) p. 434.
41. N. S. Golosov, L. E., Popov, L. W. Pudan, *J. Phys. Chem. Solids* Vol. 34, (1973) p. 1149, p. 1157.
42. R. Kikuchi, *Acta Metallurgica*, Vol. 25, (1977) p. 195.
43. S. M. Shapiro, SD Axe, G. Shifame, *Phys. Rev. B.* Vol. 6, (1972) p. 4332.
44. L. D. Landau, *Sov. Phys.* Vol. 11, (1937) p. 26, p. 545.
45. E. M. Lifshitz, *Fig. Zh.* Vol. 7, (1942) p. 61, p. 251.
46. A. G. Khachaturyan, *Progress in Materials Science*, Vol. 22, (1978) p. 1
47. L. Guttman, *J. Chem. Phys*, Vol. 34, (1961) p. 1024.
48. P. C. Clapp in Long Range Order in Solids, Academic Press Inc.
49. P. C. Clapp, *Phy. Rev. Letters*, Vol. 16, (1966) p.687.
50. J. Friedel, *Phil. Mag.* Vol. 43, (1952) p. 153.
51. J. S. Langer and S. H. Vosko, *J.P.C.S.*, Vol 12 (1959) p.186.
52. A. J. Harrison and A. Paskin, *J. Phys. Soc. Japan*, Vol. 15 (1960) p 1902.
53. F. Ducastelle and F. Gautier, *J. Phys. F.*, Vol 6 (1976), p. 2039.
54. T. L. Cottrell, The Strength of Chemical Bonds, Buttrworths Scientific Publ., London, 1854
55. V. I. Vedeneyen, et al., Bond Energies, Ionization Potentials and Electron Affinities. Edward Arnold Publ. LTD, London, 1966
56. S. C. Mass and P. C. Clapp, *Phys. Rev.*, Vol 171 (1968) p. 764.
57. S. V. Semenovskaya, *Fizika tverd, Tela.*, Vol. 9, (1967) p. 3408.
58. S. C. Moss, *J. Appl. Phys.*, Vol. 35 (1964) p. 3547.
59. S. M. Dunayevski and V. K. Nikulin, *J. Phys. F*, Vol. 12, (1982) p. L123.
60. *Metals Handbook - Ninth Edition, Volume 3*, ASM, Metals Park, OH, 1980.

END

FILMED

4-85

DTIC